Rare Metal Materials and Engineering
Volume 47, Issue 6, June 2018
Online English edition of the Chinese language journal

Available online at www.sciencedirect.com
ScienceDirect

Cite this article as: Rare Metal Materials and Engineering, 2018, 47(6): 1744-1748.

ARTICLE

Synthesis and Photoluminescence of Er^{3+} and Yb^{3+} Doped ZnS Nanocrystals

Li Lihua[1], Zhang Xiang[2], Li Xinli[1], Huang Jinliang[1], Alex A. Volinsky C[3]

[1] Henan University of Science and Technology, Luoyang 471023, China; [2] China Aviation Lithium Battery Co., Ltd, Luoyang 471000, China; [3] University of South Florida, 4202 E. Fowler Ave., ENB118, Tampa FL 33620, USA

Abstract: ZnS:Er/Yb nanocrystals were synthesized by a hydrothermal method using thioglycolic acid as a stabilizer. The crystalline phases, morphology, chemical bond states and photoluminescent properties of the nanoparticles were characterized by X-ray diffraction, transmission electron microscopy, X-ray photoemission spectroscopy and fluorescence photometer. The results show that most prepared nanoparticles are spherical in shape with an average size of 5 nm, and have cubic zinc blende crystal structure. The emission spectrum of ZnS:Er/Yb nanocrystals excited at 270 nm displays three main peaks at 470, 530 and 580 nm, and the intensity of fluorescence peaks is the strongest for nanocrystals prepared at 120 °C. When ZnS: Er/Yb nanocrystals are excited at 980 nm, the emission peaks around 540 and 650 nm appear, associated with the $^4F_{3/2}\rightarrow{}^4I_{15/2}$ and $^4F_{9/2}\rightarrow{}^4I_{15/2}$ of Er^{3+} ions transitions, respectively.

Key words: ZnS:Er/Yb nanocrystals; hydrothermal; photoluminescence

Zinc sulfide (ZnS) is an important II-VI semiconductor material and its direct band gap was reported to be 3.65 eV[1]. Due to its excellent luminescence and photochemistry properties, ZnS has been widely applied in solar cells[2], nuclear batteries[3], optoelectronic devices[4], light emitting diodes (LEDs)[5, 6] and bio-probes in sensing and imaging[7-10]. Doping is one of the most intensively used methods to modify the luminescence, electrical and optical properties of semiconducting nanomaterials by introducing traps and discrete energy states in the band gap for the excited electrons. In 1994, Bhargava et al. first demonstrated optical properties of manganese-doped ZnS nanocrystals[11], after which a large number of investigations on transition metal doped ZnS nanocrystals have been reported. Manganese-doped ZnS exhibits excellent luminescence efficiency and thermal stability, which highlight the prospects of potential applications in therapeutic and diagnostic fields[12-14]. ZnS nanorods doped with 0 mol%~15 mol% of Cu have been prepared by a simple solvothermal process[15]. Z. H. Xu et al.[3] designed, fabricated, and tested beta radioluminescence (RL) nuclear battery based on the ZnS: Cu phosphor layers with plane and V groove structures. Cr-doped ZnS nanoparticles with Cr concentrations of 0.5 at%, 1 at%, 2 at% and 3 at% were successfully synthesized by the chemical co-precipitation method using EDTA as the capping agent[16].

It is known that the rare-earth elements as dopants could be more beneficial in modifying the luminescence properties of ZnS by considering their special 4f-4f intra-shell transitions. M. Pal et al. have synthesized Eu-doped ZnS nanoparticles by a wet chemical route, and observed the red PL emission due to the intra-4f transitions of Eu^{3+} ions[17-19]. For the Tb-doped ZnS nanocrystals photoluminescence properties, the four transitions from $^5D_4\rightarrow{}^7F_6$, $^5D_4\rightarrow{}^7F_5$, $^5D_4\rightarrow{}^7F_4$ and $^5D_4\rightarrow{}^7F_3$ of Tb^{3+} ions have been reported in literature [20]. In this paper, photoluminescence properties of Er/Yb doped ZnS nanocrystals with about 5 nm in diameter obtained by a hydrothermal method with thioglycolic acid as a stabilizer were discussed.

Received date: June 09, 2017
Foundation item: National Natural Science Foundation of China (51332003-1)
Corresponding author: Huang Jinliang, Ph.D., Professor, School of Materials Science and Engineering, Henan University of Science and Technology, Luoyang 471023, P. R. China, Tel: 0086-379-642312696, E-mail: huangjl@haust.edu.cn

1 Experiment

All the reagents or solvents were of analytical grade and used without further purification. Sodium sulfide ($Na_2S·9H_2O$: 98%) and zinc acetate ($Zn(Ac)_2$: 99%) were purchased from Tianjin Kermel Chemistry Reagent Co., Ltd. Thioglycolic acid ($C_2H_4O_2S$: 99.8%) was purchased from Tianjin FuYu Chemistry Reagent Co., Ltd. Erbium nitrate ($Er(NO_3)_3·5H_2O$: 99.95%) was purchased from Shanghai PuZhen Biological Technology Co., Ltd. Ytterbium nitrate ($Yb(NO_3)_3·5H_2O$: 99.9%) was purchased from the Shanghai Purple Regent Factory.

ZnS:Er/Yb nanocrystals were prepared by the hydrothermal method. The molar ratio of sodium sulfide to zinc acetate was 1:1. Zinc acetate and doped ions with different molar ratios were dissolved in deionized water. Subsequently, thioglycolic acid ($C_2H_4O_2S$) was added in the above solution, and acted as the stabilizer with constant stirring at room temperature for 30 min. Then the solution was slowly poured into the autoclave, and synthesized for 8 h at 100, 120, 140 and 160 °C. The products were filtered, washed several times with deionized water and then with ethanol, and subsequently dried in vacuum at 60 °C. The procedure yielded a large number of ZnS:Er/Yb nanoparticles with particle size of about 5 nm. The luminescent properties of these particles were studied.

The crystalline phases of ZnS:Er/Yb nanocrystals were identified by X-ray diffraction (XRD, DX-1000, Dandong, China). The data was recorded for 2θ values ranging from 20° to 80°. The scan rate was 1°/min. The size and morphology of the nanocrystals were observed by high-resolution transmission electron microscopy (HRTEM, JEM-2010, Shimadzu, Japan). The chemical bond states were analyzed by X-ray photoemission spectroscopy (XPS, Escalab 250Xi, USA). The photoluminescence spectra of the nanocrystal samples were measured using a fluorescence spectrophotometer (F-280, Tianjin, China) and grating spectrograph (Zolix SBP-300, USA).

2 Results and Discussion

2.1 Structure analysis

X-ray diffraction patterns of Er,Yb doped ZnS nanoparticles which were synthesized at 140 °C for 8 h are shown in Fig.1. The XRD patterns of nanoparticles exhibit a cubic structure with some peaks for the (311), (220) and (111) planes. The average size (D) of the ZnS nanoparticles can be calculated according to the Scherrer's equation: $D=k\lambda/\beta\cos\theta$, where k is a constant (shape factor of about 0.89), λ is the X-ray wavelength (0.15406 nm), β is the full width at half maximum and θ is the diffraction angle. The average crystalline size of the ZnS:Er/Yb nanoparticles is estimated to be 5.2, 4.8, 5.4 and 5.6 nm.

Typical TEM, HRTEM images and selected area electron

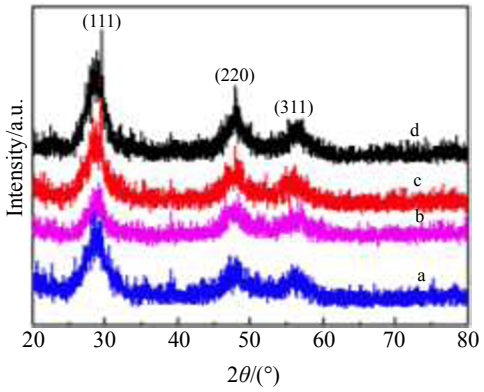

Fig.1 XRD patterns of ZnS:Er/Yb nanoparticles: (-a) ZnS:Er(1 mol%), Yb(1 mol%), (-b) ZnS:Er(1 mol%), Yb(2 mol%), (-c) ZnS:Er (1 mol%), Yb(3 mol%), and (-d) ZnS:Er (1 mol%), Yb(4 mol%)

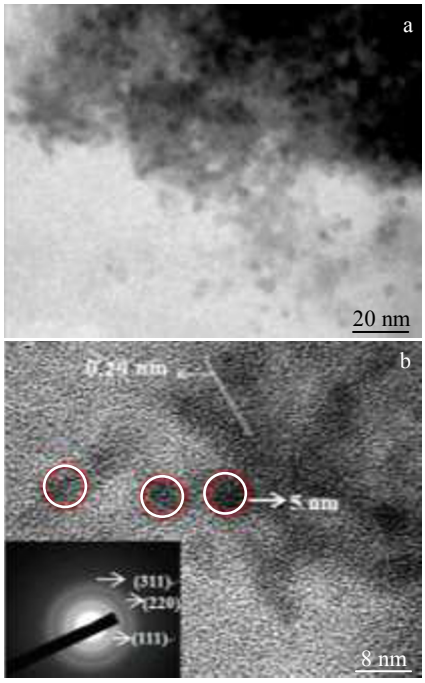

Fig.2 TEM image (a) and HRTEM image and SAED pattern (b) of ZnS:Er/Yb (2%) nanoparticles

diffraction (SAED) pattern of ZnS:Er/Yb (2%) nanocrystals are shown in Fig.2. As seen from Fig.2a, as-prepared nanoparticles are nearly spherical and the average diameter is about 5 nm, which is in agreement with the value obtained from XRD analysis. According to the SAED pattern in Fig.2b, the fringe spacing is about 0.29 nm, corresponding to the (111) crystal planes of the zinc blende ZnS. From the small inset of Fig.2b, it is also seen that the ZnS nanoparticles are polycrystalline. The (111), (220) and (311) plane rings of the SAED analysis clearly

confirm the zinc blende structure of ZnS[21].

2.2 XPS analysis

Fig.3 shows the XPS survey spectra of the product. The binding energy values are 163.3 eV for S 2p and 1022.7 eV for Zn $2p_3$, and the kinetic energy for Zn LMM is 988.7 eV. These results are consistent with the values reported by Jiang et al[22]. The amount of impurities, such as CO_2, H_2O, and O_2 adsorbed on the surface of the ZnS nanomaterials is small, as can be seen from the survey spectrum of the sample. Since XPS is a surface-sensitive technique, the XPS spectra can primarily reveal the chemical states of the outermost layers of the particles. The detailed scans of the Er 4d and Yb 4d regions are displayed in Fig.4a and 4b. It is found that most of the Er, Yb-doped sites are located near the surface of the particle.

2.3 Photoluminescence property analysis

Photoluminescence emission spectra of ZnS:Er/Yb with doped concentration of 2 mol% nanocrystals excited at 270 nm prepared at different temperatures are shown in Fig.5. The ZnS:Er/Yb nanocrystals have three strong emission peaks at 470, 530 and 580 nm. The emissions centered at 470 and 580 nm from colloidal suspensions of ZnS were assigned to vacancy and interstitial defects[23]. The peak at 530 nm is due to the transition of Er ions from the energy level $^2H_{11/2}\rightarrow{}^4I_{15/2}$. In addition, the fluorescence intensity of the ZnS:Er/Yb nanocrystals first increases and then decreases with the reaction temperature. The fluorescence peak intensity is the strongest for nanocrystals prepared at 120 °C. The enhancing ions thermal motion causes part of the fluorescence quenching as the reaction temperature increases. The fluorescence intensities of ZnS:Er/Yb nanocrystals with different Yb ions concentrations prepared at 120 °C is shown in Fig.6. The intensity of the emission peaks increases and then decreases with the doping concentration. When Er ion concentration is 1 mol%, ZnS:Er/Yb nanocrystals have the strongest performance with Yb ions doping amount of 3 mol%. It facilitates efficient energy transfer from the Yb^{3+} ions to the Er^{3+} ions in the condition.

Fig.7 indicates the emission spectra of ZnS:Er/Yb nanocrystals excited at 980 nm. The peaks around 540 and 650 nm

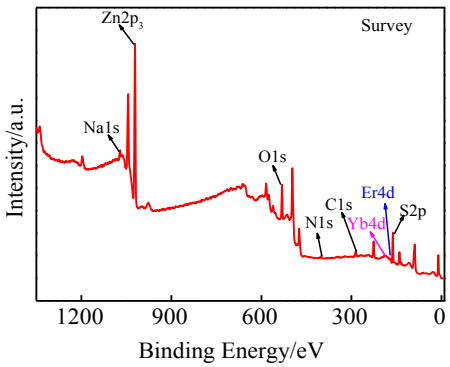

Fig.3 XPS wide survey spectrum of the ZnS:Er/Yb nanocrystals

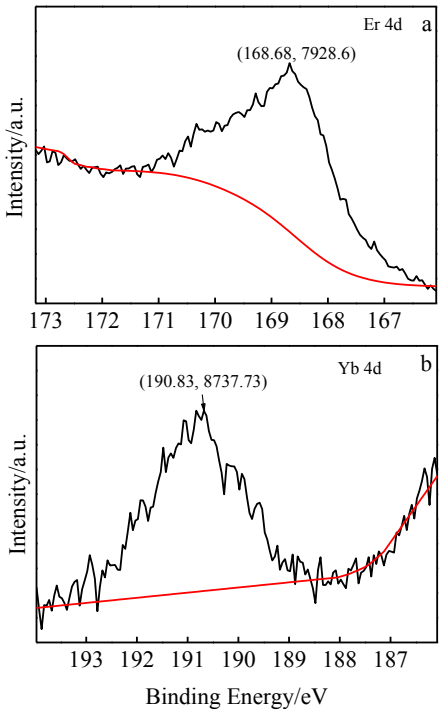

Fig.4 XPS detail scans of Er 4d (a) and Yb 4d (d) of ZnS nanocrystals

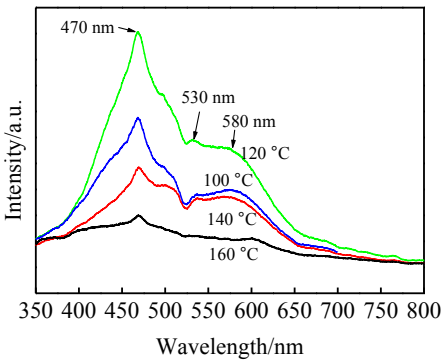

Fig.5 Emission spectra of ZnS:Er/Yb nanoparticles excited at 270 nm prepared at different temperatures

are associated with transition $^4F_{3/2}\rightarrow{}^4I_{15/2}$ and $^4F_{9/2}\rightarrow{}^4I_{15/2}$ of Er^{3+} ions, respectively. Trivalent Yb possesses an extremely simple energy level scheme with only one excited 4f level of $^2F_{5/2}$. The $^2F_{7/2}\rightarrow{}^2F_{5/2}$ transition of Yb^{3+} is well resonant with many f-f transitions of typical uncovering lanthanide ions, such as Er^{3+}. The electric dipole moment operator of the radiation results in the strongest interaction. Meanwhile, the excited Yb^{3+} ions transfer the energy to the Er^{3+} ions. The transition energy level diagram of the Yb^{3+} ions and the Er^{3+} ions is shown in Fig.8[24].

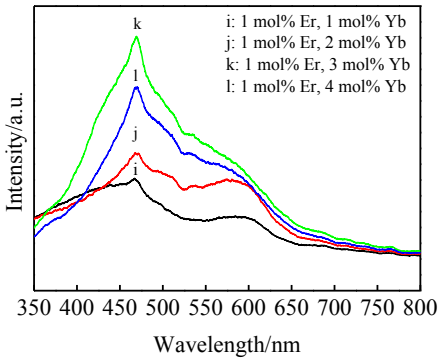

Fig.6 Emission spectra of ZnS:Er/Yb nanocrystals with different Yb ions concentrations at 120 °C

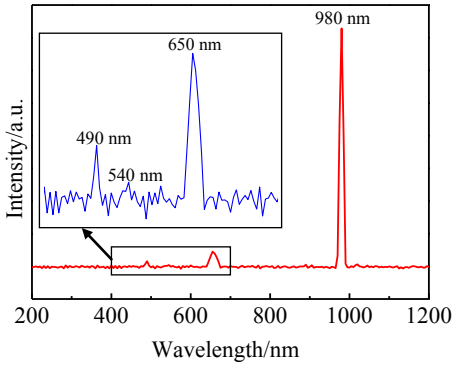

Fig.7 Emission spectra of ZnS:Er/Yb nanocrystals excited at 980 nm

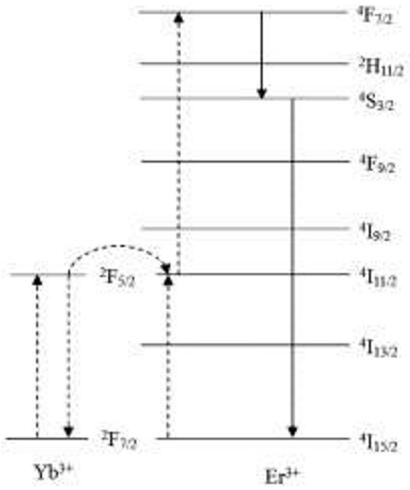

Fig.8 Energy level diagram of Yb^{3+} ions and Er^{3+} ions

3 Conclusions

1) ZnS:Er/Yb nanocrystals can be synthesized by the hydrothermal method with thioglycolic acid as a stabilizer. ZnS:Er/Yb nanoparticles have about 5 nm particle size with cubic zinc blende crystal structure.

2) The emission spectrum of the ZnS:Er/Yb nanocrystals excited at 270 nm shows three main peaks at 470, 530 and 580 nm, and the intensity of fluorescence peaks is the strongest when the nanocrystals are prepared at 120 °C. When ZnS:Er/Yb nanocrystals are excited at 980 nm, the emission peaks around 540 and 650 nm appear, associated with transition $^4F_{3/2} \rightarrow {}^4I_{15/2}$ and $^4F_{9/2} \rightarrow {}^4I_{15/2}$ of Er^{3+} ions, respectively.

References

1 Zhang Y C, Wang G Y, Hu X Y *et al*. *Materials Research Bulletin*[J], 2006, 41(10): 1817

2 Shit A, Chatterjee S, Nandi A K. *Physical Chemistry Chemical Physics*[J], 2014, 16(37): 20 079

3 Xu Z H, Tang X B, Hong L *et al*. *Journal of Radioanalytical and Nuclear Chemistry*[J], 2015, 303(3): 2313

4 Ni W S, Lin Y J. *Applied Physics A*[J], 2015, 119(3): 1127

5 Gupta S, McClure J C, Singh V P. *Thin Solid Films*[J], 1997, 299(1-2): 33

6 He X X, Wang W J, Li S H *et al*. *ECS Solid State Letter*[J], 2015, 4(2): 10

7 Geszke M, Murias M, Balan L *et al*. *Acta Biomaterials*[J], 2011, 7(3): 1327

8 Ban R, Li J J, Cao J T *et al*. *Analytical Methods*[J], 2013, 5(21): 5929

9 Augustine M S, Anas A. *Spectrochimica Acta Part A: Molecular and Biomolecular Spectroscopy*[J], 2015, 136: 327

10 Zhou W B, Swift J F, Baneyx B F. *Chemical Communications*[J], 2015, 51: 3515

11 Bhargava R N, Gallagher D, Hong X *et al*. *Physical Review Letters*[J], 1994, 72(3): 416

12 Wang H F, Wu Y Y, Yan X P. *Analytical Chemistry*[J], 2013, 85(3): 1920

13 Zhang K, Yu T, Liu F *et al*. *Analytical Chemistry*[J], 2014, 86(23): 11 727

14 Tania J B, Meriem G, Helene G D *et al*. *Journal of Nanoparticle Research*[J], 2015, 17(6): 1

15 Srivastava R K, Pandey N, Mishra S K. *Materials Science Semiconductor Process*[J], 2013, 16(6): 1659

16 Reddy D A, Murali G, Vijayalakshmi R P *et al*. *Applied Physics A*[J], 2011, 105(1): 119

17 Lotey G S, Jindal Z, Singhi V *et al*. *Materials Science Semiconductor Process*[J], 2013, 16(6): 2044

18 Ashwini K, Pandurangappa Y C. *Optical Materials*[J], 2014, 37: 537

19 Pal M, Mathews N R, Morales E R. *Optical Materials*[J], 2013, 35(12): 2664

20 Liang Z G, Mu J, Han L *et al*. *Journal of Nanomaterials*[J], http://dx.doi.org/10.1155/2015/519303

21 Mohammadikish M, Davar F, Loghman-Estarki M R. *Ceramics International*[J], 2013, 39(3): 3173

22 Jiang X C, Xie Y, Lu J *et al*. *Chemical Materials*[J], 2001, 13(4): 1213

23 Lee J C, Park D H. *Materials Letters*[J], 2003, 57(19): 2872

24 Wang F, Liu X G. *Chemical Society Review*[J], 2009, 38(4): 976